scientific reports

Check for updates

OPEN

Construction and initial validation of key gene network for progesterone resistance in endometrial cancer based on genome-wide CRISPR screening

Xinyue Li[1,2], Shourong Wang[1,2], Ziyi Qiu[1,2], Rui Sun[1,2], Tong Wang[1,2], Xiaochen Ren[1,2], Binglin Lv[3], Xiaohong Ma[4], Lei Cheng[5]✉, Yao Liu[2,6,7]✉ & Jie Jiang[1,2]✉

Endometrial carcinoma, a prevailing malignancy of the female reproductive system, exhibits escalating incidence and a trend towards early onset. Hormone therapy serves as a primary choice for fertility preservation and is also considered for advanced and recurrent cases. However, a considerable number of patients fail to respond favorably to progestin treatments. We employed CRISPR/Cas9 technology to establish a comprehensive human genome library in the Ishikawa cell line. Subsequent exposure to medroxyprogesterone was followed by high-throughput sequencing, and differential gene expression and enrichment analyses were conducted using Model-based Analysis of Genome-wide CRISPR-Cas9 Knockout (MAGeCK) Robust Rank Aggregation (RRA) and MAGeCK Maximum-Likelihood Estimation (MLE) algorithms. An iterative data intersection approach was employed, utilizing sequenced data from progestin-resistant cell lines, to identify pivotal genes associated with progestin resistance. The top 10 identified genes were functionally validated in our previously established progestin-resistant cell model through Cell Counting Kit-8 (CCK-8) assays and apoptosis detection. The progestin-resistant gene *NNMT* and the progestin-sensitive gene *SOX17* were validated in vivo in xenograft mouse models. The constructed library exhibited high quality, meeting sequencing standards. Employing RRA and MLE algorithms, we identified 332 and 829 negative selection genes, as well as 3438 and 5098 positive selection genes. Enrichment analysis implicated pathways linked to DNA and RNA synthesis, metabolism, and related processes. After multiple data intersections, we identified a total of 5 genes promoting progestin resistance and 20 genes inhibiting resistance, with functional experiments confirming their roles. Employing CRISPR/Cas9 technology enables the construction of a relatively reliable network of pivotal genes associated with progestin resistance in endometrial carcinoma. Processes involving DNA and RNA synthesis, metabolism, and related mechanisms appear to significantly impact the progestin sensitivity of endometrial carcinoma.

Keywords Endometrial cancer, Progesterone resistance, CRISPR screening

Abbreviations

MAGeCK	Model-based analysis of genome-wide CRISPR-Cas9 knockout
RRA	Robust rank aggregation
MLE	maximum-likelihood estimation

[1]Department of Gynecology and Obstetrics, Qilu Hospital of Shandong University, Jinan 250012, China. [2]Gynecologic Oncology Key Laboratory of Shandong Province, Qilu Hospital of Shandong University, Jinan 250012, China. [3]Department of Radiology, Qilu Hospital of Shandong University, 250012 Jinan, China. [4]Department of Gynecology and Obstetrics, The Affiliated Yantai Yuhuangding Hospital of Qingdao University, Yantai 264000 , China. [5]Department of Gynecology and Obstetrics, Qilu Hospital of Shandong University (Qingdao), Qingdao 266000, China. [6]Department of Gynecology, Shandong Provincial Hospital Affiliated to Shandong First Medical University, Jinan 250021, China. [7]Shandong Key Laboratory of Reproductive Research and Birth Defect Prevention, Shandong First Medical University, 250021 Jinan, China. ✉email: cl028709@qlyyqd.com; liuyao1205@foxmail.com; qljiangjie@sdu.edu.cn

CCK-8	Cell counting kit-8
EC	Endometrial cancer
EAC	Endometrial adenocarcinoma
PR	Progesterone receptor
Ish-MR	Ishikawa-medroxyprogesterone resistance cell line
CRISPR	Clustered regularly interspaced short palindromic repeats
Cas9	CRISPR-associated protein 9
gRNA	Guide RNA
TCGA	The cancer genome atlas
siRNA	Small interfering RNA

Endometrial cancer (EC) is one of the most common malignant tumors of the female reproductive system, and its incidence has been increasing year by year, showing a trend of younger age[1]. The main treatment for EC is surgery, followed by adjuvant radiotherapy and chemotherapy according to different risk stratification[2]. Unlike some solid tumors such as lung cancer and melanoma, where immunotherapy is widely used, and ovarian cancer, another malignant tumor of the female reproductive system, where PARP inhibitors have clear benefits, hormonal therapy is still an attractive treatment option for some patients with EC[3–8]. For patients with poor physical condition, progestin therapy can be used as a first-line treatment for advanced disease, or as a second-line/third-line treatment[9,10]. In addition, especially for patients with endometrial hyperplasia with atypia and early/low-risk endometrial adenocarcinoma (EAC) who have fertility requirements, hormonal conservative treatment seems to have become their first choice[11]. However, its complete response rate is only 55–76%, and about 30% of patients are insensitive to progestin therapy or develop progestin resistance during treatment[12,13]. A large number of patients cannot benefit from progestin therapy, and its clinical application still faces huge challenges.

In recent years, numerous studies have been conducted by scholars to elucidate the mechanisms of progesterone resistance in EAC. Progesterone inhibits EAC progression by binding to progesterone receptors (PRs), thereby impeding cell cycle progression, angiogenesis, and epithelial-mesenchymal transition (EMT) while promoting apoptosis[14]. Resistance to progesterone is classically attributed to aberrant PR signaling, involving mechanisms such as reduced PR expression, subtype imbalance, and epigenetic alterations[15–18]. Several other common pathways in tumors, including TGF/EGFR/MAPK, PI3K/AKT/mTOR, and those regulating EMT and oxidative stress, have also been shown to play a role in progesterone resistance[15,19–23]. Furthermore, our research group previously established a stable progesterone-resistant EAC cell line (Ishikawa-medroxyprogesterone resistance cell line, Ish-MR) through concentration gradient induction, and differential gene expression was identified through RNA sequencing. Subsequent enrichment analysis revealed that processes and pathways related to lipid metabolism, the immune system and inflammation, and the extracellular environment may play critical roles in progesterone resistance[24]. Subsequent studies have found that cholesterol and fatty acid synthesis rate-limiting enzyme SREBP-1 and monoglyceride lipase MGLL, closely associated with lipid metabolism, are highly expressed in Ish-MR cells and can induce progesterone resistance in EAC[25,26]. While there are various theories regarding progesterone resistance, the complete elucidation of its mechanisms remains an ongoing pursuit.

Clustered Regularly Interspaced Short Palindromic Repeats (CRISPR)– CRISPR-associated protein 9 (Cas9) system is a natural bacterial defense mechanism against bacteriophage infection and plasmid transfer[27]. CRISPR-mediated genome editing relies on Cas effector proteins that target specific genomic sequences of interest. Cas9 utilizes guide RNA (gRNA) composed of a constant structural scaffold and short programmable sequences called spacers to target genomic loci. It has now emerged as a powerful RNA-guided DNA targeting platform, employed for genome editing, transcriptional perturbation, epigenetic regulation, and genome imaging[28]. By using single-guide RNA (sgRNA) libraries, CRISPR-based whole-genome screening can be used to identify drug targets or disease-resistant genes. Therefore, CRISPR-Cas9-mediated genome engineering holds immense promise in the treatment and even cure of genetic diseases, including various forms of cancer, neurodegenerative disorders, and immunological conditions, among others[29–31].

Here we constructed a whole-genome library for EAC cell lines using the CRISPR-Cas9 system and performed high-throughput sequencing after drug treatment in this study. Differential gene screening and enrichment analysis were conducted using various algorithms (Fig. 1). Moreover, we identified five genes that promote drug resistance and five genes that inhibit drug resistance by intersecting differentially selected gene lists obtained through various methods. Their roles in progesterone resistance were further validated through MTT and apoptosis assays.

Methods

Genome-wide CRISPR/Cas9 screen

Genome-wide lentiviral Human_GeCKOv2_Library _B was purchased from AZENTA LIFE SCIENCES (Suzhou, China). For CRISPR screening, 1×10^8 Ishikawa (RRID: CVCL_2529) cells were infected pooled GeCKOv2 lentiviral library with functional MOI of 0.3. (All experiments were performed with mycoplasma-free cells, cell lines were tested for mycoplasma contamination every two months using the Mycoplasma PCR Detection kit (Biyuntian C0301S).) After 48 h of puromycin selection, the cells were divided into three groups, the "baseline" group cells were collected and frozen at − 80℃, the "control" group cells were treated with DMSO for 10 days while the "MPA" group cells were treated with 15 μM MPA for 10 days. Genomic DNA from each group was isolated using HMW DNA Kit (740160.20, MACHEREY-NAGEL, Germany) and amplified by PCR. The PCR products were purified and subjected to NGS by using the Novaseq 6000-PE150 platform (AZENTA LIFE SCIENCES, China).

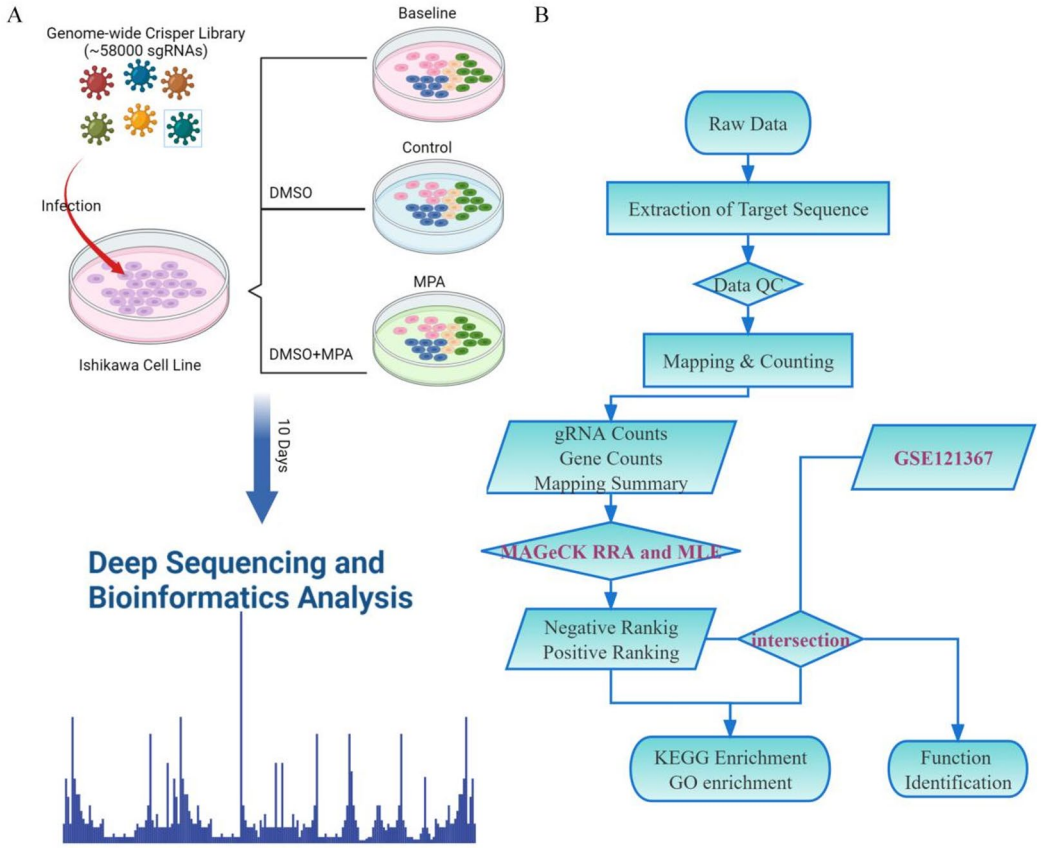

Fig. 1. Conceptual and workflow diagram of the study. (**A**) Cell line treatment and library construction process. (**B**) Sequencing data analysis and gene selection verification workflow.

Quality control and differential gene selection

Quality control and preliminary screening

The target sgRNAs were extracted and subjected to quality control using an in-house script. The Model-based Analysis of Genome-wide CRISPR-Cas9 Knockout (MAGeCK) software was utilized to align the sgRNAs to the sgRNA library, perform differential gene selection, and conduct KEGG/GO enrichment analysis. "MAGeCKFlute" was used to analyze CRISPR genetic screens, and MAGeCK Robust Rank Aggregation (RRA) and MAGeCK Maximum-Likelihood Estimation (MLE) were performed to identificate the CRISPR-screen hits in this flow. MAGeCK RRA utilizes RRA enrichment scores to indicate the importance of genes, and the "beta score" was calculated by MAGeCK MLE to measure the degree of selection when perturbing the gene[32]. We define the negatively selected genes as drug-resistant genes and the positively selected genes as drug-sensitive genes. In the RRA screening, genes with a defined *p*-value less than 0.05 are considered as differentially expressed genes. We used MAGeCK (Version 0.5.7) and MAGeCKFlute (Version 0.5.7) in R v4.0.3. RRA outputs are reported with nominal p and BH-FDR (q), and hits were considered at $q < 0.10$ unless otherwise noted. MLE results are summarized by $\Delta\beta$ effect sizes for direction and magnitude, serving as a complementary ranking metric rather than a significance test.

Screen genes for validation

The data from GSE121367 was standardized using R. Genes were defined as differentially expressed if they had a *p*-value less than 0.05 and an absolute log2 fold change (LogFc) greater than or equal to 2. Subsequently, the differentially expressed genes were sorted in descending order based on the absolute LogFc values, and then separated into two groups: the high-expression group (drug-resistant genes) and the low-expression group (drug-sensitive genes). Further filtering is performed by taking the intersection of the results obtained from RRA and MLE. The new gene list maintains the order of genes as they appear in the MLE screening results. Finally, the intersection of the top half of drug-resistant and drug-sensitive genes from the aforementioned intersection is further intersected with the corresponding top half of genes from GSE121367, which will be used for subsequent analysis and functional validation.

Gene expression and survival analysis

The RNA-sequencing data (level 3) and corresponding clinical information from 544 patients with uterus carcinoma were collected from The Cancer Genome Atlas (TCGA) dataset (https://portal.gdc.cancer.gov/). The data acquisition and application followed the recommended guidelines and policies. To assess the survival

difference between the two groups, Kaplan-Meier survival analysis with log-rank tests was conducted. Kaplan-Meier curves, *p*-values, and hazard ratios (HR) with 95% confidence intervals (CI) were generated using log-rank tests and univariate Cox proportional hazards regression. All the aforementioned analytical methods and R packages were implemented with R software version v4.0.3 (The R Foundation for Statistical Computing, 2020). A significance level of $p < 0.05$ was considered statistically significant.

Functional validation of selected genes

The effects of these genes on progestin sensitivity in endometrial cancer were validated by measuring the IC50 and apoptosis levels of the Ish-MR cell line after separately inhibiting drug resistance-promoting genes and overexpressing drug sensitivity-promoting genes. As the representatives of drug resistance-promoting and sensitivity-promoting genes, the effects of *NNMT* and *SOX17* were validated in xenograft models.

Plasmid construct and transfection

The coding sequence of *NNMT*, *HHIPL*, *KCNRG*, *SOX17*, *RPL22L1* and *ZIC2* was cloned into pcDNA3.1 plasmid. Small interfering RNA (siRNA) of *PDE1A*, *NNMT*, *DTX3L*, *AMPD3* and *ABCC2* was synthesized by RiboBio. Plasmids and siRNAs were transfected into cells using lipo2000 reagent (Invitrogen; Thermo Fisher Scientific, Waltham, MA, USA). RNA and protein were extracted 48–72 h after transfection. The sequence of siRNAs were shown in SupTable 1.

Western blot

Total protein was extracted by ultrasonic lysis of RIPA buffer, protein concentration was measured by BCA method. A total of 15–30 μg protein was used to perform SDS-PAGE electrophoresis per lane. Then protein was transferred to PVDF membranes and blocked with 5% nonfat milk. Then membrane was incubated by primary antibodies and secondary antibodies. The ECL system was used to detect the expression of protein. The antidodies of SOX17(A18858), RPL22L1(A23204), ZIC2(A15736), PDE1A(A10457), NNMT(A23786), DTX3L(A18551), AMPD (A6354) and ABCC2(A8405) were from ABclonal. The antidodies of HHIPL(sc-515618) and KCNRG(sc-390290) were purchased from Santa Cruz Biotechnology (Dallas, TX, USA). The experimental samples were blinded to the experimental operator.

qPCR

Total RNA was extracted by FastPure Cell/Tissue Total RNA Isolation Kit (RC101, Vazyme). RNA was reverse transcribed as cDNA. qPCR was performed using cDNA as a template. The relative expression of genes was calculated by ΔΔCt method. The primer sequences were listed in SupTable 2. The experimental samples were blinded to the experimental operator.

Cell viability

Cell viability was measured by Cell Counting Kit-8 (CCK8-kit). In brief, cells were seeded in 96-well plates and exposed to different concentration of MPA for 48 h. 100μL of fresh culture medium containing 10μL of CCK-8 solution was added to each well and incubation for 4 h. The absorbance at 450 nm was quantified by a microplate spectrophotometer. Data from CCK-8 assays are expressed as the mean ± SD from three independent experiments. Statistical differences were analyzed by one-way ANOVA with Dunnett's multiple comparisons test. The IC50 values were derived from nonlinear regression and compared between cells using an unpaired t-test. $P < 0.05$ was considered significant.

Flow cytometry

Cells were collected and stained using FITC Annexin V Apoptosis Detection kit (556547, BD Biosciences, USA) as manufacturer's instructions. Then cells were detected by flow cytometry with three independent biological replicates. CytExpert (2.4.0.28) software was used to analyze the flow cytometry data.

Tumor xenograft model

This study was approved by the Research Ethics Committee of Qilu Hospital of Shandong University (KYLL-202210-055-1). All animal procedures were performed in accordance with the relevant guidelines and regulations.The four-week-old female BALB/c nude mice were randomly divided into four groups ($n = 5$) using a stratified randomization method: Group 1 received Ish-PCMV-Ctrl cell implantation and DMSO; Group 2 received Ish-PCMV-Ctrl cell implantation and MPA; Group 3 received Ish-PCMV-NNMT cell implantation and DMSO; Group 4 received Ish-PCMV-NNMT cell implantation and MPA. The mice were injected with 1×10^7 tumor cells subcutaneously and treated with intraperitoneal injection of drugs every other day after tumor formation. For MPA, the dose was 100 mg/kg/ bodyweight[25,33] and the control group received the same amount of DMSO. Tumor size = width^2 × length/2. After the sacrifice of the mice, tumor weight was measured. And we established four additional groups with IshMR-PCMV-Ctrl cells and IshMR-PCMV-SOX17 cells. All other parameters were identical to those previously described.

Results

The sequencing quality control of the samples is qualified

After filtering, all three sample groups yielded valid read counts exceeding 24,000,000, representing approximately 95% of the original read count. The proportion of bases with sequencing quality values greater than 20 was over 98% of the total bases, and bases with sequencing quality values exceeding 30 accounted for over 95% of the total bases. The average error rate for all bases was 0.02%. The median gRNA sequencing depth was around 370, and the average number of lost gRNAs in the gRNA library among the three samples was 5. The library coverage for

all samples was 99.99%. The gRNA library corresponded to a total of 19,834 genes, with only one gene remaining undetected in the Control group (Table 1 and SupFigure 1).

Differential genes were identified using the RRA algorithm

The RRA algorithm is primarily employed for comparing two experimental conditions and can identify significantly selected sgRNAs and their corresponding genes between these conditions. The use of RRA enrichment scores facilitates the ranking of differentially expressed genes, where lower RRA scores indicate greater importance in cellular growth[32,34]. After filtering and sorting based on a significance threshold of $P < 0.05$, a total of 332 negatively selected genes and 3438 positively selected genes were identified. The top ten genes based on RRA scores, for negative selection, are *KAL1*, *GPX4*, *NXF5*, *CLEC4F*, *COQ10B*, *CCR9*, *RDH16*, *RNMT*, *YME1L1*, and *NNMT*. For positive selection, the top ten genes are *ATP6V1G1*, *SIN3A*, *DET1*, *ATP6V0C*, *GINS1*, *WDR55*, *BRF1*, *ZNRD1*, *LOC100288332*, and *FOXD4L2*. Their distribution and weights are depicted in Fig. 2A-B. Subsequent Gene Set Enrichment Analysis (GSEA) revealed enrichment of GO pathways including Rna metabolic process, Cytoplasmic translation, Site of double-strand break, Chromosome, telomeric region, Translation initiation factor activity (Fig. 2C). Additionally, KEGG pathways such as Dna replication, Rna polymerase, Mismatch repair, Basal transcription factors, Nucleotide excision repair, and Homologous recombination were enriched (Fig. 2D)[35–37], as determined by GSEA analysis.

Differential genes were identified using the MLE algorithm

MLE is an analytical modeling method suitable for complex experimental designs. It enables the analysis of data from various conditions, as in the case of typical drug screening experiments involving at least three conditions:

SampleID		Baseline	MPA treatment	Control
Sequencing quality	Raw reads	25,240,962	26,167,956	25,710,382
	Raw bases(G)	7.57	7.85	7.71
	Clean reads	24,046,198	24,821,110	24,255,587
	Clean bases(G)	0.48	0.5	0.49
	Effective rate(%)	95.27	94.85	94.34
	Q20(%)	98.66	98.56	98.45
	Q30(%)	95.98	95.69	95.41
	Error rate(%)	0.02	0.02	0.02
	GC ration(%)	54.44	54.21	54.16
Comparison information	Read	24,046,198	24,821,110	24,255,587
	Mappedreads	22,527,777(93.69%)	23,162,120(93.32%)	22,556,693(93.00%)
	Grna_mean_depth	396	407	396
	Max_depth	17,016	20,072	17,846
	Median_depth	369	378	366
	Totalgrnas	56,869	56,869	56,869
	Zerogrnas	4	5	6
	Coverage_rate	99.99%	99.99%	99.99%
	Totalgenes	19,834	19,834	19,834
	Zerogenes	0	0	1
	Giniindex	0.05885	0.05838	0.06206

Table 1. Statistical data of sequencing quality and sample comparison information. Raw_reads: Raw number of reads; Raw_base(G): Raw base number; Clean_reads: Read counts after filtration; Clean_base(G): Base counts after filtration; Effective rate(%): The ratio of clean reads to raw reads; Q20(%): Proportion of the total bases with a sequencing quality value greater than 20(Generally above 90%); Q30(%): Proportion of the total bases with a sequencing quality value greater than 30(Generally above 80%); Error rate(%): Average error rate for all bases; GC ratio(%): The total content of GC bases; Read: gRNA read counts; MappedReads: Full Alignment of Reads to the gRNA Library; Grna_mean_depth: Average Sequencing Depth of gRNAs, calculated as the total number of gRNA reads aligned to the reference sequence divided by the number of gRNAs in the aligned gRNA Library; Max_depth: Maximum Sequencing Depth of gRNAs, referring to the number of alignments for the gRNA in the gRNA Library with the highest number of reads aligned among all gRNAs; Median_depth: Median Sequencing Depth of gRNAs; Totalgrnas: Total number of gRNAs in the gRNA library; Zerogrnas: Number of missing gRNAs in the gRNA library; Coverage_rate: Library coverage, defined as the proportion of detected gRNAs out of the total gRNAs(For library quality control, a coverage of > 90% is typically required); Totalgenes: Total number of genes targeted by the gRNA library; Zerogenes: Number of genes that were not detected; GiniIndex: Average abundance of gRNAs, with values between 0 and 1 (Average abundance of gRNAs, with values between 0 and 1. A smaller value indicates a more uniform distribution of sequencing reads across gRNAs, typically less than 0.1).

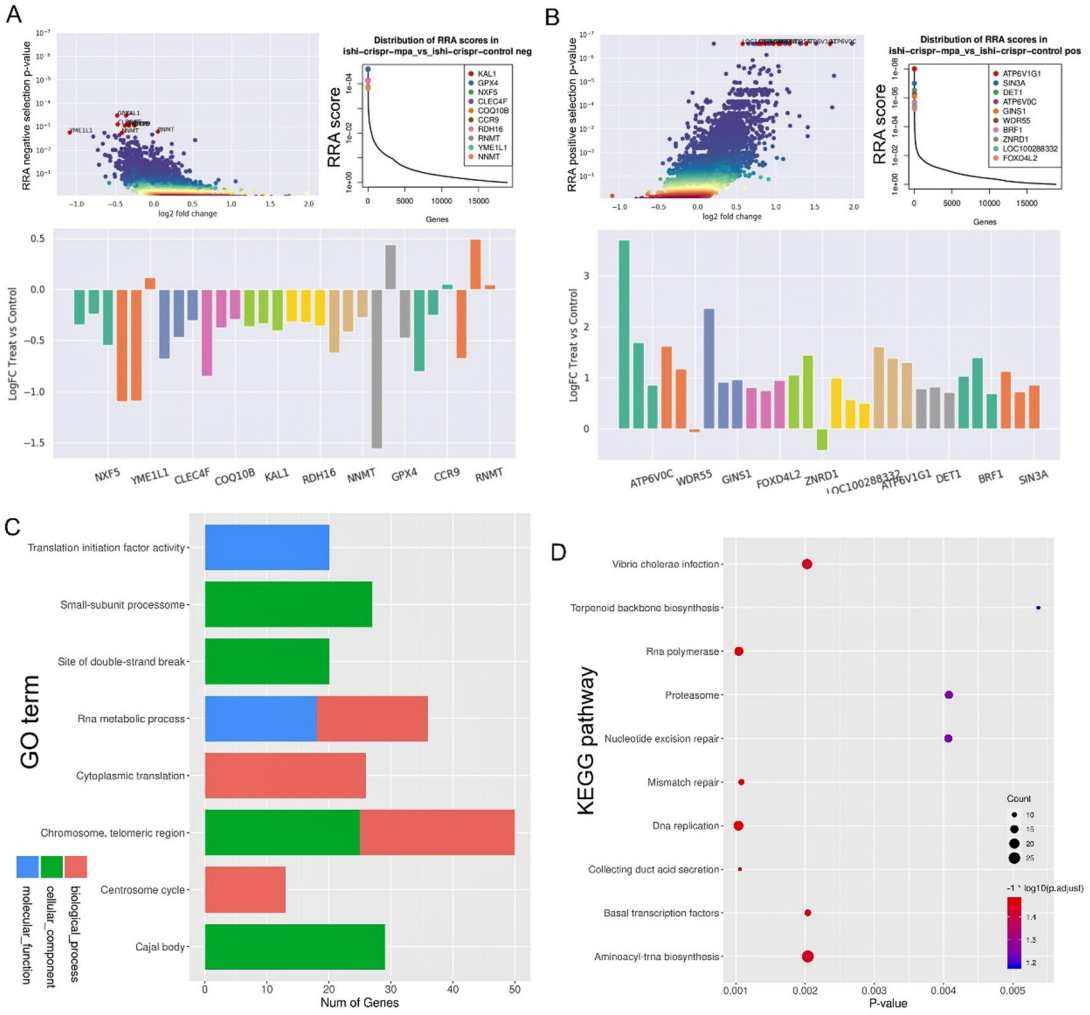

Fig. 2. Differential genes selected by RRA and GSEA. (**A**) Volcano plot of negative select genes, distribution of RRA scores of negative select genes and LogFC distribution of top 10 genes in negative selection. Each bar represents one sgRNA, showing the effect size and direction (depletion or enrichment) in treatment compared to control. (**B**) Volcano plot of positive select genes, distribution of RRA scores of positive select genes and LogFC distribution of top 10 genes in positive selection. Each bar represents one sgRNA, showing the effect size and direction (depletion or enrichment) in treatment compared to control. (**C**) GO analysis of differential genes selected by RRA. (**D**) KEGG analysis of differential genes selected by RRA. Pathway enrichment analysis was performed using KEGG database resources[35–37].

blank control, vector or drug solvent treatment control, and drug treatment conditions[32]. MLE computes a "β score" for each target gene to measure the extent of gene perturbation, akin to the "log fold change" measurement in differential expression analysis. The Delta Beta Score (treatment group beta score minus control group beta score) is used for ranking differentially expressed genes. Scatter plots and differential gene rankings based on the Delta Beta Score are presented in Figs. 3A-B. In this study, a total of 829 negatively selected genes and 5098 positively selected genes were identified. The top 10 negatively selected genes are *FAM3C*, *YME1L1*, *KRT86*, *LRRC37B*, *DNAF1*, *FAM126B*, *CACNA1D*, *CLEC4F*, *COQ10B*, and *KCTD3*. The top 10 positively selected genes are *ATP6V0C*, *ST20-MTHFS*, *SPDYE5*, *ATP6V1G1*, *ARL17B*, *MBD3L4*, *GINS1*, *RPL13*, *SART3*, and *PRC1*. GSEA results show enrichment in GO pathways, including Chromosome, telomeric region, Cytoplasmic translation, Rna metabolic process, Positive regulation of gene expression, epigenetic, Cajal body, and Translation initiation factor activity (Fig. 3C), similar to the earlier RRA section. Similarly, KEGG pathways such as Nucleotide excision repair, Basal transcription factors, Dna replication, Rna polymerase, Mismatch repair, and Homologous recombination were also enriched (Fig. 3D)[35–37].

Key genes were further selected through the integration of Ish-MR sequencing results

We intersected the negative screening gene sets of RRA and MLE, resulting in a total of 240 genes (Fig. 4A). Similarly, the intersection of the positive screening gene sets of RRA and MLE yielded a total of 3064 genes (Fig. 4B). Subsequently, we further intersected the top 1/2 of these two sets with the top 1/2 of the pro-resistance

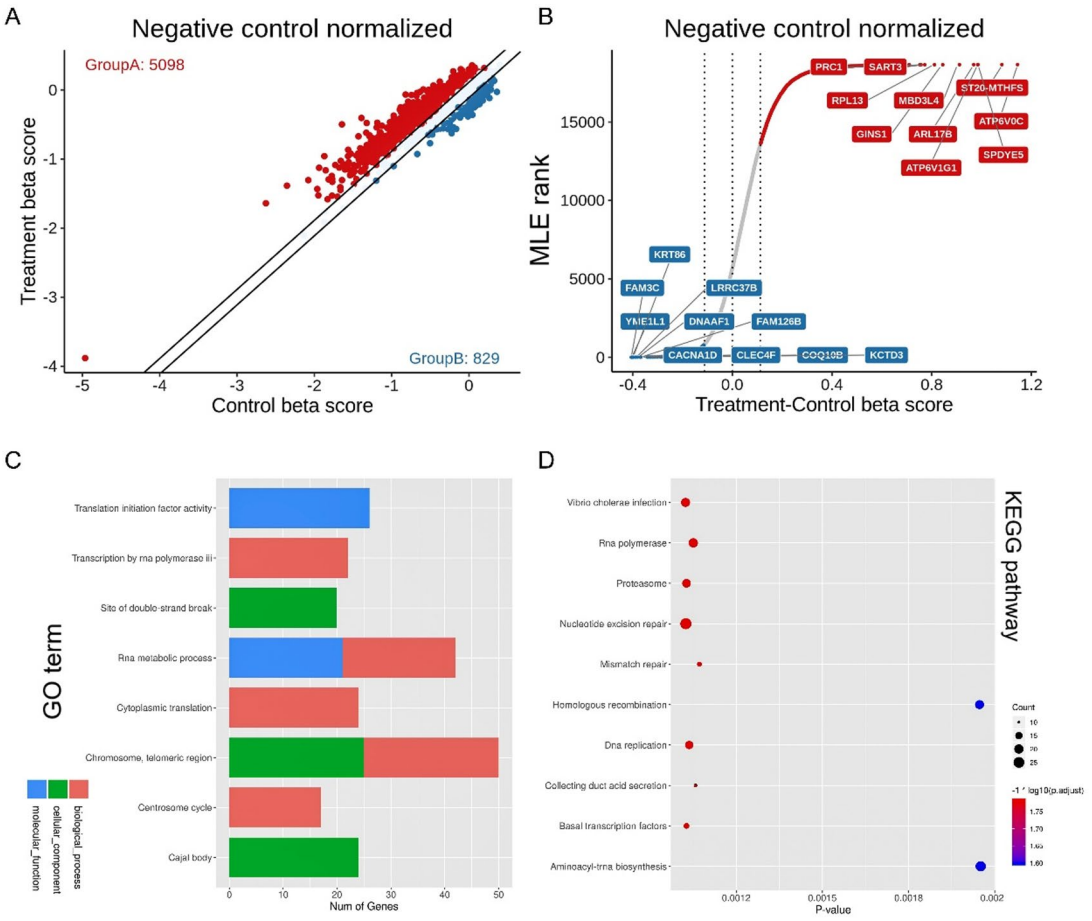

Fig. 3. Differential genes selected by MLE and GSEA. (**A**) Dot plot of beta value distribution. Group A refers to positive selected genes by MLE, and Group B refers to negative selected genes by MLE. (**B**) Delta beta score ranks of genes selected by MLE. Red refers to positive selected genes, and blue refers to negative selected genes. (**C**) GO analysis of differential genes selected by MLE. (**D**) KEGG analysis of differential genes selected by RRA. Pathway enrichment analysis was performed using KEGG database resources[35–37].

and anti-resistance gene sets from the GSE121367 dataset, leading to the identification of 5 key pro-resistance genes and 20 anti-resistance genes (Fig. 4C). The top 5 ranked genes from each set were chosen for subsequent analysis and validation. Expression analysis using the TCGA database revealed that, overall, pro-resistance genes show relatively low mRNA expression levels in EC samples, whereas anti-resistance genes tend to be more highly expressed. Further analysis demonstrated that most (4 out of 5) of the pro-resistance genes showed no significant differences in expression across different pathological types. On the other hand, a significant increase in expression was observed for the majority (4 out of 5) of anti-resistance genes in EAC compared to serous carcinoma and mixed-type carcinoma (SupFigure 2 A-B). Gene expression correlation analysis revealed that the expression of *PGR*, progesterone membrane receptors (*PGRMC1*, *PGRMC2*, *PAQR7*, *PAQR8*), estrogen receptors (*ESR1*, *ESR2*) and *ESRRG* was positively correlated with most of the 10 genes, with sifgnificant correlations observed especially for *PGRMC1*, *PGRMC2*, *ESR1*, and *ESRRG* (P<0.001) (SupFigure 2 C). *ESRRB* also showed strong positive correlations with *PDE1A*, *ABCC2* and *DTX3L*. In contrast, *NNMT* expression is weakly negatively correlated with *PGR* and *ESR1*. This may reflect that mRNA levels do not equate to protein function, and progesterone resistance involves mechanisms beyond PR expression alone, which are consistent with the findings of previous clinical studies[38,39]. Survival analysis indicated a significant association between high expression of *AMPD3* and *KCNRG* and unfavorable prognosis, whereas elevated expression of *DTX3L* was associated with a favorable prognosis (SupFigure 2D-E).

Manipulation of selected genes can effectively reverse progesterone resistance

We performed transfections and rescue experiment using siRNA and overexpression plasmids for the previously identified 5 pro-resistance and 5 anti-resistance genes. This allowed us to observe the impact of these manipulations on the progesterone sensitivity of the Ish-MR. The results demonstrated that all 10 genes could be effectively knocked down or overexpressed (SupFigure 3). Upon knocking down the pro-resistance genes or overexpressing the anti-resistance genes, Ish-MR cells exhibited a significant increase in apoptosis and a marked decrease in the IC50 value after progesterone treatment (Figs. 5 and 6). These findings provide

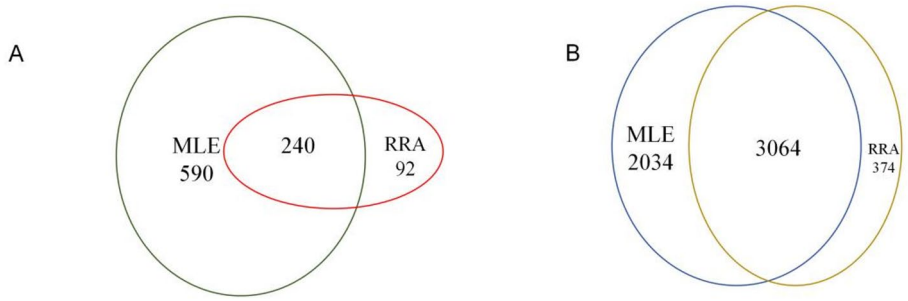

C

The intersection of the first 1/2 of each queue

Promoting drug resistance		Promoting drug sensitivity		
NNMT	SOX17	PGF	MXRA5	C3orf14
PDE1A	ZIC2	TMEM170B	ANGPTL2	CGREF1
ABCC2	KCNRG	LRCH2	DLX5	TSTD1
DTX3L	HHIPL1	CDH18	TNC	SALL2
AMPD3	RPL22L1	RADIL	DDX43	WNT3A

Fig. 4. Genes selected via intersection of different sets. (**A**) The 240 genes were selected via intersection of RRA and MLE negative selections. (**B**) The 3064 genes were selected via intersection of RRA and MLE positive selections. (**C**) The 5 candidate drug-resistant genes were selected through two rounds of intersections, and the 5 genes within the blue box were selected for further functional validation. (**D**) The 20 candidate drug-sensitive genes were selected through two rounds of intersections, and the top 5 genes have been highlighted with a red box and selected for further functional validation.

conclusive evidence that the manipulation of these genes led to an enhancement in progesterone sensitivity. In an in vivo context, Ishikawa and IshMR cell xenograft models were established and treated with DMSO or MPA respectively. It was found that compared with the control groups, overexpression of *NNMT* enhanced progesterone resistance in Ishikawa cells, while overexpression of *SOX17* promoted progesterone sensitivity in Ish-MR cells (Fig. 7, SupFigure 4).

Discussion

Endometrial cancer (EC) remains a major challenge in gynecologic oncology, particularly for young patients seeking fertility preservation. Progestin-based therapies, including oral progesterone and LNG-IUD, are widely used for early-stage and recurrent EC. However, their clinical efficacy is limited—complete remission rates in early-stage EC rarely exceed 70–80%[40,41], and the overall response rate (ORR) for progesterone treatment in advanced and recurrent EC patients is only about 30%[42]. The emergence of progesterone resistance has therefore become a major obstacle to successful conservative and systemic treatment, underscoring the urgent need to elucidate its molecular mechanisms and identify new therapeutic targets.

With this in mind, researchers have made tremendous efforts to explore the mechanisms underlying progesterone resistance in EC and have attempted to develop therapeutic strategies to reverse this resistance. Inhibitors of the PI3K/AKT/mTOR pathway, for example, can enhance the therapeutic effect of progesterone by increasing PR protein or PR messenger RNA expression. Epigenetic regulators, such as DNA methyltransferase inhibitors and histone deacetylase inhibitors, can reverse progesterone resistance by reducing methylation of the PR promoter and restoring functional PR expression. Additionally, certain psychiatric drugs, like chlorpromazine, may increase the expression of PRB to enhance progesterone sensitivity[43–48]. Furthermore, our research group discovered that the *SREBP1* inhibitor Fatostatin can reverse progesterone resistance by inhibiting the SREBP1-NF-κB pathway, and the *MGLL* inhibitor ABX-1431 can reverse progesterone resistance as well[25,26]. In summary, progesterone itself regulates various mechanisms through PRs and its A and B isoforms to achieve therapeutic effects in EC[49]. However, it is also posited that the emergence of progesterone resistance is not solely dependent on aberrations in PR expression, especially in studies concerning endometriosis[50,51]. In this study, although genes such as *PGR*, *PGRMC1*, and *PGRMC2* appeared in the list of positively screened genes, they were not situated in pivotal positions. Moreover, the PCR results following the manipulation of target genes demonstrated that the expression patterns of these progesterone receptor-associated genes did not fully correlate with the resistant phenotype (SupFigure 5). Previous studies mostly focused on exploring the function and mechanisms of individual genes/pathways in progesterone sensitivity. In the early stages of this project, we performed transcriptome sequencing on constructed Ish-MR to screen for resistance-related genes. However, with

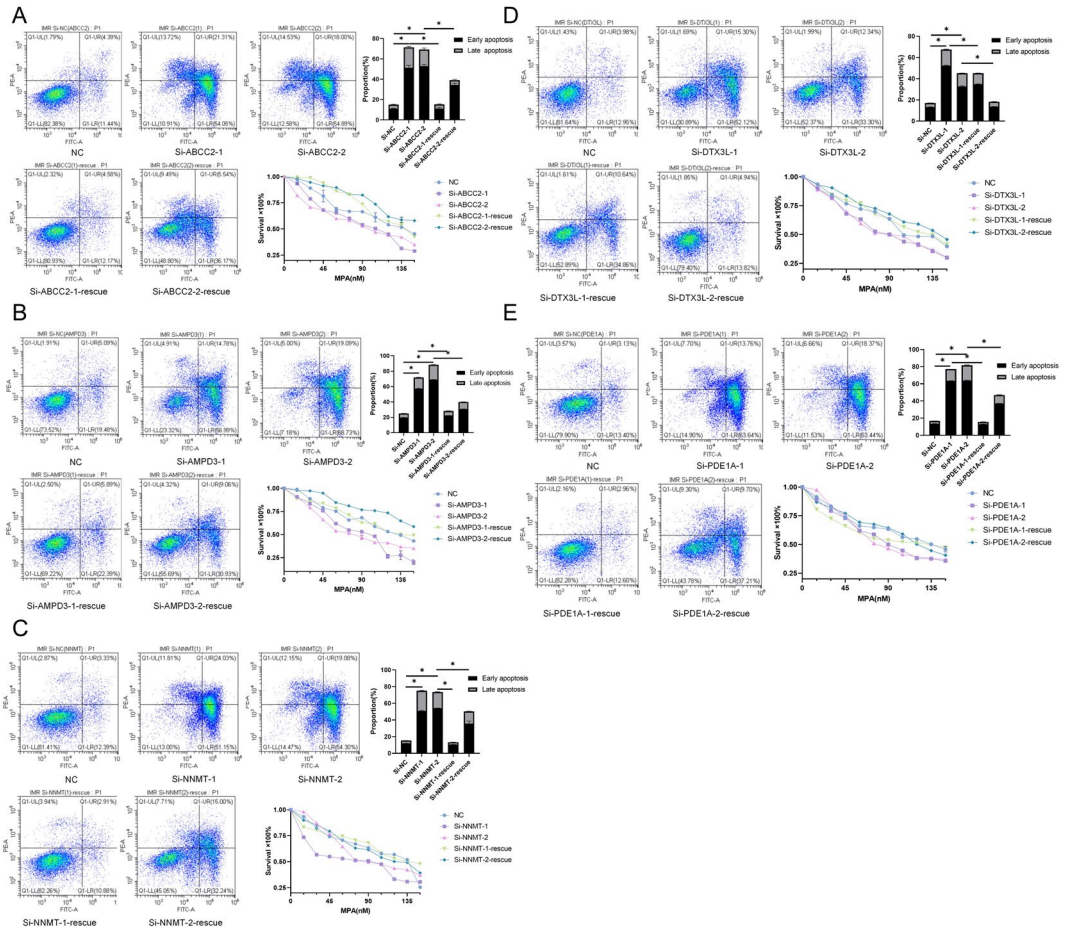

Fig. 5. Changes in sensitivity of Ish-MR to MPA after interference with drug-resistant genes. (**A**) Following the knockdown of ABCC2 expression using various siRNA sequences and subsequent rescue overexpression, Ish-MR cells were assessed for MPA drug concentration inhibition curves and apoptosis detection via flow cytometry. The IC50 values were determined to be 138.6, 96.9, 96.3, 135.0, and 167.18 μM, respectively. (**B**) Similar experimental interventions on AMPD3. The IC50 values were determined to be 130.8, 88.7, 76.4, 139.1, and 183.5 μM, respectively. (**C**) Similar experimental interventions on NNMT. The IC50 values were determined to be 119.2, 66.5, 87.8, 145.1, and 120.8 μM, respectively. (**D**) Similar experimental interventions on DTX3L. The IC50 values were determined to be 119.9, 87.5, 88.0, 128.0, and 142.1 μM, respectively. (**E**) Similar experimental interventions on PDE1A. The IC50 values were determined to be 136.4, 91.5, 80.8, 124.8, and 123.6 μM, respectively. (The IC50 value was calculated from three independent biological replicates ($n = 3$) using the "Quest Graph™ IC50 Calculator" (AAT Bioquest, Inc., https://www.aatbio.com/tools/ic50-calculator). The apoptosis data are presented as the mean ± SD of three independent biological replicates ($n = 3$). Error bar refers to mean and SD. $^*P < 0.05$.)

advancements in gene-editing technology, CRISPR-Cas9 library screening has been utilized for drug-related gene selection, offering greater accuracy and efficiency compared to traditional gene screening methods[34,52]. In this study, we employed CRISPR-Cas9 whole-genome library to screen genes related to progesterone resistance in EAC, revealing some previously unfamiliar genes and pathways that play a role in this process. Recently, Wang et al. also used CRISPR library screening to identify *ADCK3* as a key gene involved in MPA resistance and conducted in-depth validation[53]. In contrast, our study focused more on utilizing various algorithms to construct a broader and comprehensive MPA resistance network. Moreover, the list of differentially expressed genes we obtained still exhibits significant discrepancies compared with theirs, which may be attributed to variations in culture conditions and screening procedures.

Our findings suggest that the resistance to MPA may involve processes associated with DNA and RNA. Pathways closely related to DNA and RNA synthesis, metabolism, and transcription, such as DNA replication, RNA polymerase, basal transcription factors, and nucleotide excision repair, were enriched, indicating that MPA resistance may depend on the initial stages. Individual differences originating from DNA and RNA stages might also contribute to the occurrence of MPA resistance. Additionally, pathways like mismatch repair and homologous recombination, which are widely mentioned in gynecologic malignancies, were also enriched. Studies have indicated that *BRCA1/BRCA2* mutation carriers exposed to higher levels of estrogen and progesterone may be related to defects in steroid progestin regulation[54].

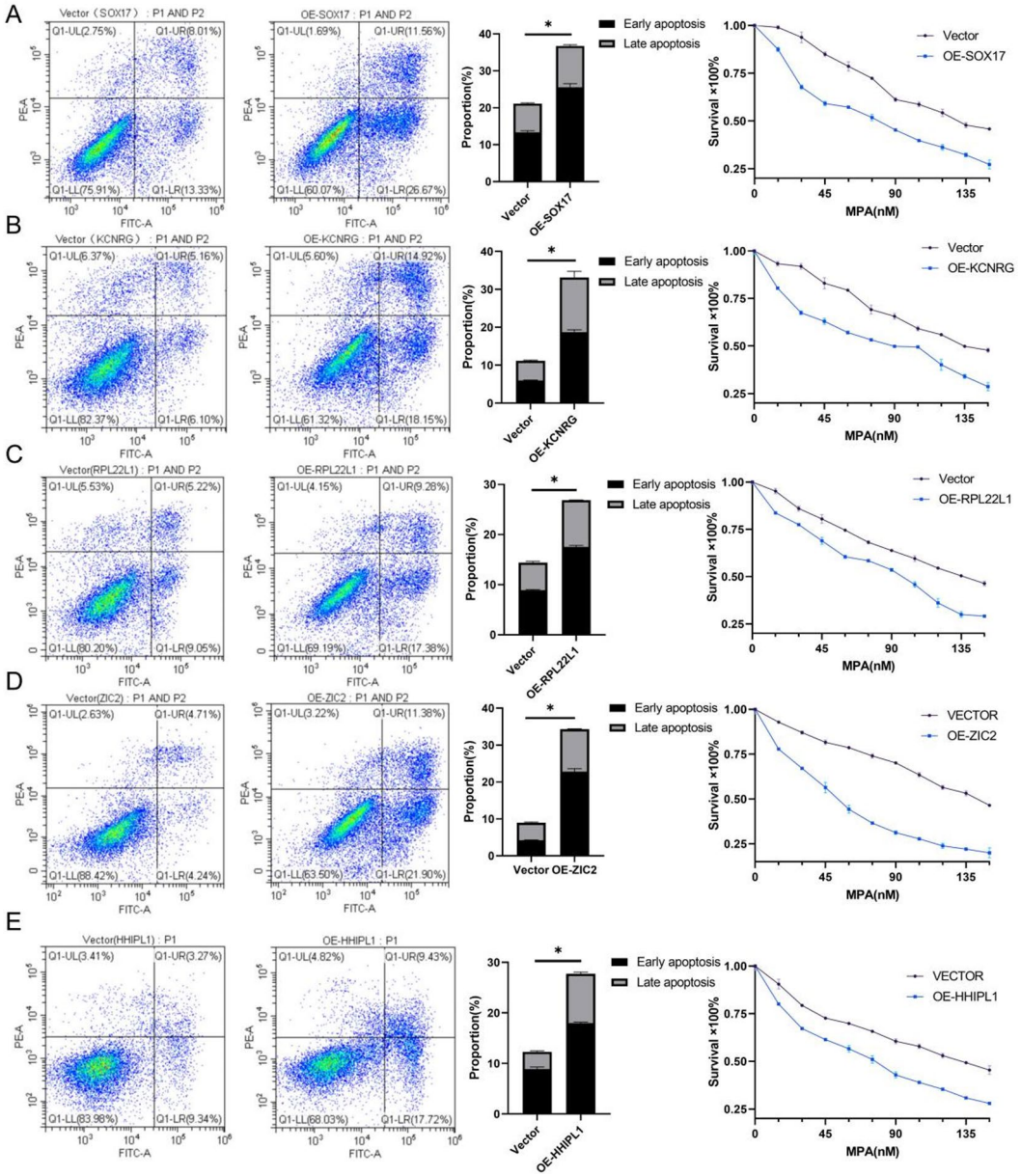

Fig. 6. Changes in sensitivity of Ish-MR to MPA after overexpression of drug-sensitive genes. (**A**) (From left to right) Drug concentration inhibition curve of Ish-MR cells towards MPA after plasmid overexpression of SOX17 and results of flow cytometry apoptosis detection. The IC50 values before and after overexpression are 130.94μM and 73.53μM, respectively. (**B**) Images are in the same order as mentioned above. The IC50 values for KCNRG overexpression were 138.28μM before overexpression and 82.41μM after overexpression. (**C**) Images are in the same order as mentioned above. The IC50 values for RPL22L1 overexpression were 136.77μM before overexpression and 89.16μM after overexpression. (**D**) Images are in the same order as mentioned above. The IC50 values for ZIC2 overexpression were 143.14μM before overexpression and 50.90μM after overexpression. (**E**) Images are in the same order as mentioned above. The IC50 values for HHIPL1 overexpression were 132.65μM before overexpression and 72.75 μM after overexpression (*$P < 0.05$. The IC50 values were calculated using the "Quest Graph™ IC50 Calculator" (AAT Bioquest, Inc., https://www.aatbio.com/tools/ic50-calculator)).

Furthermore, clinical research has shown that the mismatch repair status affects the response to fertility-sparing treatment in EC[55], suggesting that such pathways may serve as predictive markers for treatment response to some extent.

In this study, we employed various algorithms and intersected the lists of genes associated with promoting and inhibiting resistance to screen the top 5 genes from each group for validation. The results from in vitro and in vivo experiments were all in line with our expectations, and among them, *NNMT* and *SOX17* were the representatives. *NNMT* is closely related to metabolic disorders and tumors. Research

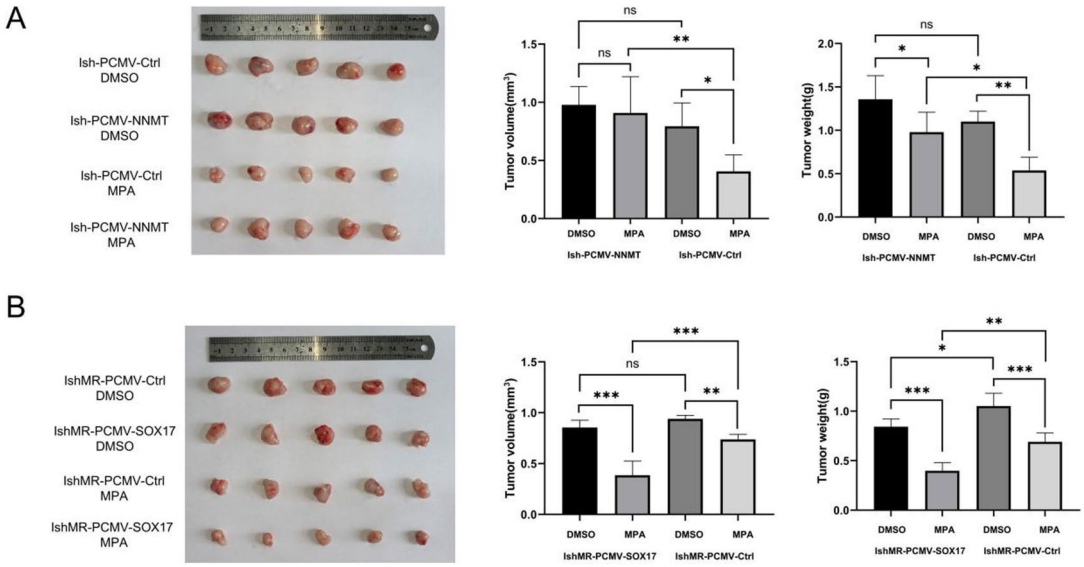

Fig. 7. The effects of NNMT and SOX17 overexpression on tumors growth in vivo. (**A**) In vivo xenograft experiments to evaluate the effects of NNMT overexpression on tumor growth. (**B**) In vivo xenograft experiments to evaluate the effects of SOX17 overexpression on tumor growth.

suggests that *NNMT* may serve as a target for treating obesity and type II diabetes[56]. Proteomic studies have revealed that *NNMT* plays a central role in cancer-associated fibroblast (CAF) differentiation and metabolic regulation in the tumor microenvironment[57]. On the other hand, *SOX17* has been proven to play a significant role in the development of EC. Independent follow-up studies confirmed that low/loss of *SOX17* expression is associated with poor prognosis, advanced cancer stage, high-grade tumors, and low recurrence-free survival rate[58]. Furthermore, *SOX17* has been shown to play an important role in ovarian cancer and cervical cancer as well[59,60]. The functional experiments conducted in this study have yielded results that are consistent with our expectations, and supported the proposed pro-resistance or anti-resistance roles of the genes we selected. While we won't elaborate on the introduction of more genes, it's important to note that further mechanistic research and exploration of applications are still worth expecting. For instance, Ibudilast, a relatively non-selective PDE inhibitor, has been studied for its potential in preventing chemotherapy-induced neurotoxicity[61], but its application in EC remains unexplored. This class of inhibitors or activators may hold promising roles in future clinical applications.

One concern of this study is that functional validation was performed mainly in a single endometrial cancer cell line, which may not fully capture tumor heterogeneity. Another limitation is the relatively small number of biological replicates. Future studies using multiple models and larger sample sizes will be needed to confirm and extend our findings. In addition, future studies should further investigate the mechanistic roles of DNA and RNA synthesis–related pathways identified in this study, as these processes appear to be closely linked to progesterone resistance. It should also be noted that some of the findings presented here are primarily correlative, and additional experimental validation will be necessary to establish direct causal relationships.

In conclusion, through CRISPR/Cas9 whole-genome library drug screening, we have established a preliminary progesterone-resistant gene network in EAC (based on the Ishikawa cell line). The results indicate that processes such as DNA and RNA synthesis and metabolism play a crucial role in progestin resistance. Furthermore, our subsequent functional experiments further validated the reliability of the screening network. This study can provide potential clinical implications by highlighting novel candidate genes and pathways that could serve as predictive biomarkers or therapeutic targets. The findings can serve as a reference for preclinical research, especially in the development of drugs aimed at reversing progesterone resistance. Incorporating these insights into future translational studies may contribute to more precise and effective management of progesterone-resistant endometrial cancer.

Data availability

The datasets of this study are included within the article and the supplementary files, and part of the raw sequencing data generated in this study have been deposited in the NCBI GEO and under the accession number of GSE121367 (https://www.ncbi.nlm.nih.gov/geo/query/acc.cgi?acc=GSE121367) and GSE241070 (https://www.ncbi.nlm.nih.gov/geo/query/acc.cgi?acc=GSE241070).

Received: 28 September 2024; Accepted: 13 January 2026
Published online: 03 March 2026

References

1. Siegel, R. L., Giaquinto, A. N. & Jemal, A. Cancer statistics, 2024. *Cancer J. Clin.* **74**(1), 12–49 (2024).
2. Haight, P. J. et al. Molecular characterization of mixed-histology endometrial carcinoma provides prognostic and therapeutic value over morphologic findings. *NPJ Precision Oncol.* **9**(1), 41 (2025).
3. Maio, M. et al. Pembrolizumab in microsatellite instability high or mismatch repair deficient cancers: Updated analysis from the phase II KEYNOTE-158 study. *Ann. Oncol.* **33**(9), 929–938 (2022).
4. Reck, M. et al. Five-Year outcomes with pembrolizumab versus chemotherapy for metastatic non-small-cell lung cancer with PD-L1 tumor proportion Score ≥ 50. *J. Clin. Oncol.* **39**(21), 2339–2349 (2021).
5. Banerjee, S. et al. Maintenance Olaparib for patients with newly diagnosed advanced ovarian cancer and a BRCA mutation (SOLO1/GOG 3004): 5-year follow-up of a randomised, double-blind, placebo-controlled, phase 3 trial. *Lancet Oncol.* **22**(12), 1721–1731 (2021).
6. Monk, B. J. et al. Niraparib first-line maintenance therapy in patients with newly diagnosed advanced ovarian cancer: final overall survival results from the PRIMA/ENGOT-OV26/GOG-3012 trial. *Ann. Oncol. Off. J. Eur. Soc. Med. Oncol.* **35**(11), 981–992 (2024).
7. Wakelee, H. et al. Perioperative pembrolizumab for early-stage non-small-cell lung cancer. *N. Engl. J. Med.* **389**(6), 491–503 (2023).
8. DiSilvestro, P. et al. Overall survival with maintenance Olaparib at a 7-Year Follow-Up in patients with newly diagnosed advanced ovarian cancer and a BRCA mutation: the SOLO1/GOG 3004 trial. *J. Clin. Oncol. Off. J. Am. Soc. Clin. Oncol.* **41**(3), 609–617 (2023).
9. Suzuki, Y. et al. Fertility-preserving treatment for stage IA endometrial cancer: A systematic review and meta-analysis. *Am. J. Obstet. Gynecol.* **231**(6), 599–610e17 (2024).
10. Hu, Z. et al. Proteogenomic insights into early-onset endometrioid endometrial carcinoma: Predictors for fertility-sparing therapy response. *Nat. Genet.* **56**(4), 637–651 (2024).
11. Fernandez-Montoli, M. E. et al. Fertility-sparing treatment for atypical endometrial hyperplasia and endometrial cancer. *Cochrane Database Syst. Rev.* **7**(7), Cd013111 (2025).
12. Baker, J., Obermair, A., Gebski, V. & Janda, M. Efficacy of oral or intrauterine device-delivered progestin in patients with complex endometrial hyperplasia with atypia or early endometrial adenocarcinoma: a meta-analysis and systematic review of the literature. *Gynecol. Oncol.* **125**(1), 263–270 (2012).
13. Contreras, N-A., Sabadell, J., Verdaguer, P., Julià, C. & Fernández-Montolí, M-E. Fertility-Sparing approaches in atypical endometrial hyperplasia and endometrial cancer patients: current evidence and future directions. *Int. J. Mol. Sci.* **23**(5), 2531 (2022).
14. Lv, M. et al. Progestin resistance and corresponding management of abnormal endometrial hyperplasia and endometrial carcinoma. *Cancers (Basel)*. **14**(24), 6210 (2022).
15. Marquardt, R. M., Kim, T. H., Shin, J-H. & Jeong, J-W. Progesterone and Estrogen signaling in the endometrium: what goes wrong in endometriosis? *Int. J. Mol. Sci.* **20**(15), 3822 (2019).
16. Yang, S. et al. Systematic dissection of the mechanisms underlying progesterone receptor downregulation in endometrial cancer. *Oncotarget* **5**(20), 9783–9797 (2014).
17. Upson, K. et al. Biomarkers of progestin therapy resistance and endometrial hyperplasia progression. *Am. J. Obstet. Gynecol.* **207**(1), 36.e1–.e8 (2012).
18. Sasaki, M. et al. Progesterone receptor B gene inactivation and CpG hypermethylation in human uterine endometrial cancer. *Cancer Res.* **61**(1), 97–102 (2001).
19. Zhou, Q. et al. DACH1 suppresses epithelial to mesenchymal transition (EMT) through Notch1 pathway and reverses progestin resistance in endometrial carcinoma. *Cancer Med.* **8**(9), 4380–4388 (2019).
20. Lin, Q., Chen, H., Zhang, M., Xiong, H. & Jiang, Q. Knocking down FAM83B inhibits endometrial cancer cell proliferation and metastasis by Silencing the PI3K/AKT/mTOR pathway. *Biomed. Pharmacother.* **115**, 108939 (2019).
21. Wang, S. et al. Mechanisms involved in the evolution of progestin resistance in human endometrial hyperplasia–precursor of endometrial cancer. *Gynecol. Oncol.* **88**(2), 108–117 (2003).
22. Al-Sabbagh, M., Lam, E. W. F. & Brosens, J. J. Mechanisms of endometrial progesterone resistance. *Mol. Cell. Endocrinol.* **358**(2), 208–215 (2012).
23. Ai, Z. et al. Overexpressed epidermal growth factor receptor (EGFR)-induced progestin insensitivity in human endometrial carcinoma cells by the EGFR/mitogen-activated protein kinase signaling pathway. *Cancer* **116**(15), 3603–3613 (2010).
24. Li, W. et al. Comprehensive bioinformatics analysis of acquired progesterone resistance in endometrial cancer cell line. *J. Transl. Med.* **17**(1), 58 (2019).
25. Ma, X. et al. ABX-1431 inhibits the development of endometrial adenocarcinoma and reverses progesterone resistance by targeting MGLL. *Cell Death Dis.* **13**(12), 1067 (2022).
26. Ma, X. et al. Fatostatin reverses progesterone resistance by inhibiting the SREBP1-NF-κB pathway in endometrial carcinoma. *Cell Death Dis.* **12**(6), 544 (2021).
27. Charpentier, E., Doudna, J. A. & Biotechnology Rewriting a genome. *Nature* **495**(7439), 50–51 (2013).
28. Jiang, F. & Doudna, J. A. CRISPR-Cas9 structures and mechanisms. *Annu. Rev. Biophys.* **46**, 505–529 (2017).
29. Barrangou, R. & Doudna, J. A. Applications of CRISPR technologies in research and beyond. *Nat. Biotechnol.* **34**(9), 933–941 (2016).
30. Heidenreich, M. & Zhang, F. Applications of CRISPR-Cas systems in neuroscience. *Nat. Rev. Neurosci.* **17**(1), 36–44 (2016).
31. Xiong, X., Chen, M., Lim, W. A., Zhao, D. & Qi, L. S. CRISPR/Cas9 for human genome engineering and disease research. *Annu. Rev. Genomics Hum. Genet.* **17**, 131–154 (2016).
32. Wang, B. et al. Integrative analysis of pooled CRISPR genetic screens using MAGeCKFlute. *Nat. Protoc.* **14**(3), 756–780 (2019).
33. Sun, R. et al. Extracellular matrix stiffness in endometrial cancer: driving progression and modulating treatment sensitivity via the ROCK1/YAP1 axis. *Cell Death Dis.* **16**(1), 380 (2025).
34. Li, W. et al. MAGeCK enables robust identification of essential genes from genome-scale CRISPR/Cas9 knockout screens. *Genome Biol.* **15**(12), 554 (2014).
35. Kanehisa, M. & Goto, S. KEGG: Kyoto encyclopedia of genes and genomes. *Nucleic Acids Res.* **28**(1), 27–30 (2000).
36. Kanehisa, M. Toward Understanding the origin and evolution of cellular organisms. *Protein Sci. Publ. Protein Soc.* **28**(11), 1947–1951 (2019).
37. Kanehisa, M., Furumichi, M., Sato, Y., Matsuura, Y. & Ishiguro-Watanabe, M. KEGG: biological systems database as a model of the real world. *Nucleic Acids Res.* **53**(D1), D672–d7 (2025).
38. Lv, M. et al. Progestin resistance and corresponding management of abnormal endometrial hyperplasia and endometrial carcinoma. *Cancers* **14**(24), 6210 (2022).
39. van Weelden, W. J. et al. The effect of progestin therapy in advanced and recurrent endometrial cancer: A systematic review and meta-analysis. *BJOG: Int. J. Obstet. Gynecol.* **130**(2), 143–152 (2023).
40. Park, J-Y. et al. Long-term oncologic outcomes after fertility-sparing management using oral progestin for young women with endometrial cancer (KGOG 2002). *Eur. J. Cancer.* **49**(4), 868–874 (2013).
41. Gunderson, C. C., Fader, A. N., Carson, K. A. & Bristow, R. E. Oncologic and reproductive outcomes with progestin therapy in women with endometrial hyperplasia and grade 1 adenocarcinoma: a systematic review. *Gynecol. Oncol.* **125**(2), 477–482 (2012).
42. van Weelden, W. J. et al. The effect of progestin therapy in advanced and recurrent endometrial cancer: A systematic review and meta-analysis. *BJOG* **130**(2), 143–152 (2023).

43. Cui, Y. et al. Chlorpromazine sensitizes Progestin-Resistant endometrial cancer cells to MPA by upregulating PRB. *Front. Oncol.* **11**, 665832 (2021).
44. Yang, S. et al. Epigenetic modification restores functional PR expression in endometrial cancer cells. *Curr. Pharm. Des.* **20**(11), 1874–1880 (2014).
45. Boumber, Y. & Issa, J-P-J. Epigenetics in cancer: what's the future? *Oncol. (Williston Park).* **25**(3), 220 (2011).
46. Gu, C. et al. Inhibiting the PI3K/Akt pathway reversed progestin resistance in endometrial cancer. *Cancer Sci.* **102**(3), 557–564 (2011).
47. Pant, A. et al. Inhibition of AKT with the orally active allosteric AKT inhibitor, MK-2206, sensitizes endometrial cancer cells to progestin. *PLoS One*. **7**(7), e41593 (2012).
48. Oza, A. M. et al. Phase II study of Temsirolimus in women with recurrent or metastatic endometrial cancer: a trial of the NCIC clinical trials group. *J. Clin. Oncol.* **29**(24), 3278–3285 (2011).
49. McGlorthan, L., Paucarmayta, A., Casablanca, Y., Maxwell, G. L. & Syed, V. Progesterone induces apoptosis by activation of caspase-8 and calcitriol via activation of caspase-9 pathways in ovarian and endometrial cancer cells in vitro. *Apoptosis* **26**(3–4), 184–194 (2021).
50. Bulun, S. E., Yildiz, S., Adli, M. & Wei, J-J. Adenomyosis pathogenesis: insights from next-generation sequencing. *Hum. Reprod. Update* **27**(6), 1086–1097 (2021).
51. McKinnon, B., Mueller, M. & Montgomery, G. Progesterone resistance in endometriosis: an acquired property? *Trends Endocrinol. Metab.* **29**(8), 535–548 (2018).
52. Matboli, M. et al. Identification of novel insulin resistance related CeRNA network in T2DM and its potential editing by CRISPR/Cas9. *Int. J. Mol. Sci.* **22**(15), 8129 (2021).
53. Zhang, Z., Zhang, M., Zhou, J. & Wang, D. Genome-wide CRISPR screening reveals ADCK3 as a key regulator in sensitizing endometrial carcinoma cells to MPA therapy. *Br. J. Cancer*. **129**, 601–611 (2023).
54. Widschwendter, M. et al. The sex hormone system in carriers of BRCA1/2 mutations: A case-control study. *Lancet Oncol.* **14**(12), 1226–1232 (2013).
55. Chung, Y. S. et al. Mismatch repair status influences response to fertility-sparing treatment of endometrial cancer. *Am. J. Obstet. Gynecol.* **224**(4), 370–e1 (2021).
56. Kraus, D. et al. Nicotinamide N-methyltransferase knockdown protects against diet-induced obesity. *Nature* **508**(7495), 258–262 (2014).
57. Eckert, M. A. et al. Proteomics reveals NNMT as a master metabolic regulator of cancer-associated fibroblasts. *Nature* **569**(7758), 723–728 (2019).
58. Tan, D. S., Holzner, M., Weng, M., Srivastava, Y. & Jauch, R. SOX17 in cellular reprogramming and cancer. *Semin. Cancer Biol.* **67**(Pt 1), 65–73 (2020).
59. Lin, L. et al. SOX17 and PAX8 constitute an actionable lineage-survival transcriptional complex in ovarian cancer. *Oncogene* **41**(12), 1767–1779 (2022).
60. Li, L., Yang, W-T., Zheng, P-S. & Liu, X-F. SOX17 restrains proliferation and tumor formation by down-regulating activity of the Wnt/β-catenin signaling pathway via trans-suppressing β-catenin in cervical cancer. *Cell Death Dis.* **9**(7), 741 (2018).
61. Teng, C. et al. Ibudilast for prevention of oxaliplatin-induced acute neurotoxicity: A pilot study assessing preliminary efficacy, tolerability and Pharmacokinetic interactions in patients with metastatic Gastrointestinal cancer. *Cancer Chemother. Pharmacol.* **86**(4), 547–558 (2020).

Acknowledgements

This study acknowledges the generous support from the Gynecologic Oncology Key Laboratory of Shandong Province.

Author contributions

Xinyue Li was responsible for data analysis, manuscript revising, experimental design and operation. Shourong Wang was responsible for manuscript writing, experimental design and operation. Ziyi Qiu, Rui Sun, Tong Wang and Xiaochen Ren assisted with experimental operations and check the data. Binglin Lv and Xiaohong Ma managed and examined the data. Yao Liu was responsible for data analysis, figure creation, and manuscript writing. Jie Jiang and Lei Cheng conceived the study concept and supervised the project.

Funding

The study was supported by National Key Technology Research and Development Programme of China (2022YFC2704304) and China Postdoctoral Science Foundation (2023M731847).

Declarations

Competing interests

The authors declare no competing interests.

Ethics approval and consent to participate

This study doesn't involve any human participants, human data or human tissue. This study was approved by the Research Ethics Committee of Qilu Hospital of Shandong University. (KYLL-202210-055-1). All procedures involving nude mice were performed in accordance with institutional guidelines and national regulations on the care and use of laboratory animals. The study is reported in accordance with the ARRIVE guidelines.

Consent for publication

Not applicable.

Additional information

Supplementary Information The online version contains supplementary material available at https://doi.org/10.1038/s41598-026-36534-x.

Correspondence and requests for materials should be addressed to L.C., Y.L. or J.J.